Exp Astron
DOI 10.1007/s10686-015-9441-6

ORIGINAL ARTICLE

Ground-based tests of JEM-EUSO components at the Telescope Array site, "EUSO-TA"

The JEM-EUSO Collaboration ·
Yoshiya Kawasaki · Lech Wiktor Piotrowski

Received: 28 October 2014 / Accepted: 16 January 2015

Abstract We are conducting tests of optical and electronics components of JEM-EUSO at the Telescope Array site in Utah with a ground-based "EUSO-TA" detector. The tests will include an engineering validation of the detector, cross-calibration of EUSO-TA with the TA fluorescence detector and observations of air shower events. Also, the proximity of the TA's Electron Light Source will allow for convenient use of this calibration device. In this paper, we report initial results obtained with the EUSO-TA telescope.

Keywords JEM-EUSO · EUSO-TA · Telescope array · Ultra high energy cosmic rays

1 Introduction

EUSO-TA is a ground-based testing campaign for the *Extreme Universe Space Observatory on-board the Japanese Experiment Module* (JEM-EUSO) [1].

The EUSO-TA aims to install a fully functional prototype of JEM-EUSO at Black Rock Mesa, the site of one of the fluorescence light detectors of the Telescope Array (TA) experiment [2]. From there it will observe artificial light from TA calibration beams as well as events coming from cosmic rays, simultaneously with the TA, allowing for calibration of the detector response and reduction of the systematic uncertainties of the measurements. The studies of the transversal profile of the shower

Contribution to the special issue 'JEM-EUSO' of Experimental Astronomy

Y. Kawasaki · L. W. Piotrowski (✉)
RIKEN, 2-1 Hirosawa, Wako-shi, Japan
e-mail: lech.piotrowski@riken.jp

Y. Kawasaki
e-mail: yoshiya@riken.jp

Published online: 08 May 2015

will be performed on a sector of a shower, with spatial resolution better than that of the TA fluorescence detector (TA-FD).

The EUSO-TA telescope consists of a refractive optical system incorporating two 1 m^2 square Fresnel lenses, focusing the light in a $\pm 6°$ field of view on one Photo-Detector Module (PDM) of 2304 pixels. The detail of the telescope is described in Section 2. When a 10^{18} eV cosmic ray shower comes to the field of view of EUSO-TA, the measurements are performed after receiving a trigger from TA-FD. The detail of the shower observation is discussed in Section 3.4.

2 EUSO-TA telescope

The EUSO-TA lenses are fabricated from UV transmitting polymethyl-methacrylate (PMMA). The baseline design of the optics is shown in Fig. 1 along with simulated spot diagrams for off-axis angles of 0°, 2°, 4° and 6°.

The 17 cm × 17 cm PDM in the focus is composed of 36 Multi-Anode Photomultiplier Tubes (MAPMTs) [3] containing 64 anodes, for a total of 2304 pixels (Fig. 2, left). The PDMs also contain a front-end ASIC [4], a 1st-level trigger FPGA board, High Voltage (HV) and HV switches. The PDM is controlled by the Data Processing (DP) box. The DP box consists of a 2nd-level trigger board [5], CPU board, Clock board, GPS board, house keeping board and low voltage power supply [6] (Fig. 2, right).

The telescope is installed in a housing located in front of the Black Rock Mesa Fluorescence Detector station of TA (Fig. 3). The location satisfies the following conditions:

1. Signals from the calibration beams (Section 3.3) of TA are observable within our field of view.

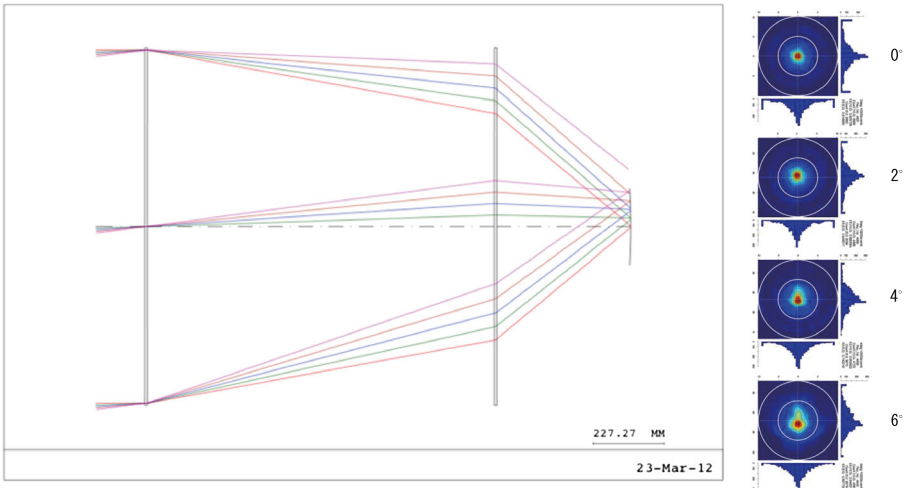

Fig. 1 The design of the EUSO-TA Optics. The left and right panels show the ray trace and spot diagrams for different incident off-axis angles, 0°, 2°, 4° and 6°, respectively

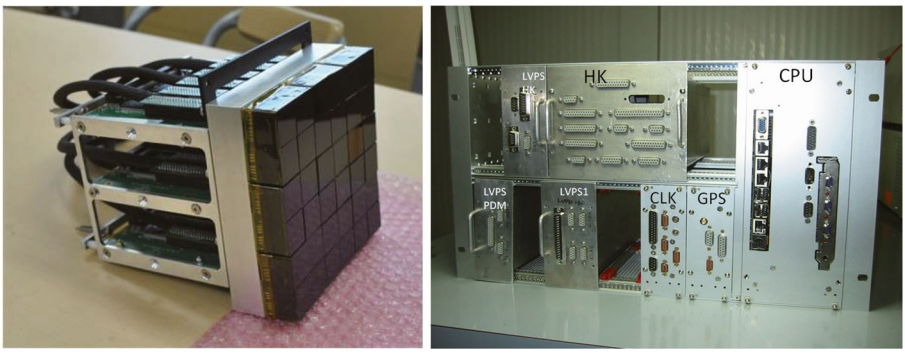

Fig. 2 The PMT array and the front-end ASIC boards mounted on the PDM frame (left) and the DP box (right). The 2nd-level trigger broad, CPU board, Clock board, GPS board, house keeping board and low voltage power supply are in the DP box

2. The housing does not obscure the field of view and/or observation of TA-FD operation.
3. Access to power, grounding, Ethernet and the TA-FD trigger signal is present.

3 Calibration and observation

3.1 Laboratory calibration

The EUSO-TA PDM consists of Hamamatsu R11265-03-M64 MAPMTs, each consisting of 64 pixels. An absolute calibration [7] is needed for obtaining the number

Fig. 3 EUSO-TA (front) and TA-FD station (back)

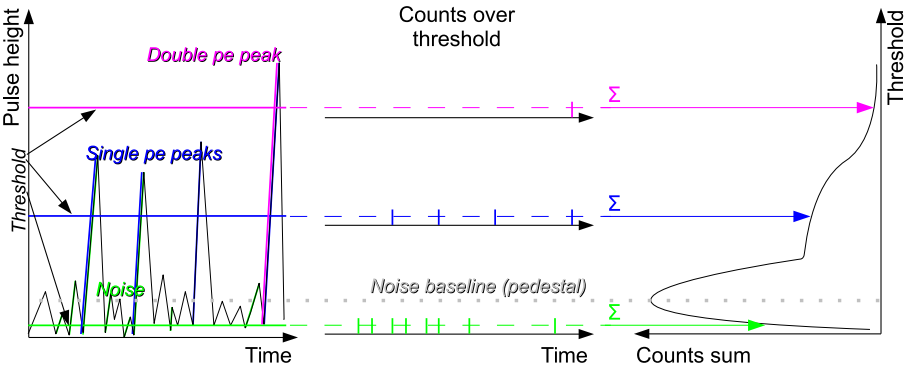

Fig. 4 A schematic dependency of signal measurement and S-curve. Right shows a schematic S-curve – sum of photon counts for specific number of measurements over the threshold for single photoelectron detection, left shows a signal change with time and the middle shows the counts – detection of pulses exceeding the thresholds. Small fluctuations are due to electronic noise, while big peaks is a single photoelectron signal, and the biggest peak is a small contribution of a double photoelectrons

of real photons hitting a pixel from the number of registered counts. This process requires estimating the spatial sensitivity of each pixel of the detector. In general it can be assumed that the sensitivity is constant in time. This, together with the complexity of this part of calibration and its time requirements, makes it a preparatory off-line task performed only once.

The goal of the "on-line calibration", which will be repeated *in-situ* between the measurements, is to obtain a similar overall performance for the single photon detection for all apparatus' pixels. In general we want to reject the noise from PMT and EC-ASIC electronics and accept more intense signal coming from a single photon. This requires analysis of so called S-curves – explained below – obtained in the process. This is the main computational task for data analysis of CPU – an iterative process of sending commands and acquiring data from lower level subsystems.

An S-curve contains Digital to Analogue Converter (DAC) signal over threshold for single photoelectron detection. To obtain it CPU requests measurement of a high number of frames for each threshold setting, to minimize statistical fluctuations[1] (Fig. 4). The pedestal peak shows the baseline of the noise, which is non-zero due to dark current and offset in readout electronics. The rising slope of the pedestal is due to triggering on a rising slope of the signal.[2] Increasing threshold above the pedestal quickly cuts off the noise. If the threshold value is above the noise but far from the typical single photoelectron signal value, the slope of the S-curve is very gentle. It steepens when the threshold crosses the typical single photoelectron signal and

[1]The actual number of frames requested for each threshold level has yet to be determined, but initial measurements show that the single photoelectron signal should be lower then 1 % of the maximal signal, requiring more then 10000 GTUs

[2]To trigger on a rising slope, the initial signal must be below the threshold value. Therefore, for thresholds below the pedestal value the detection is performed when the signal fluctuates below the threshold value and then comes back to the baseline. Therefore lowering the threshold value in this range cuts the negative fluctuations causing a drop in number of detections

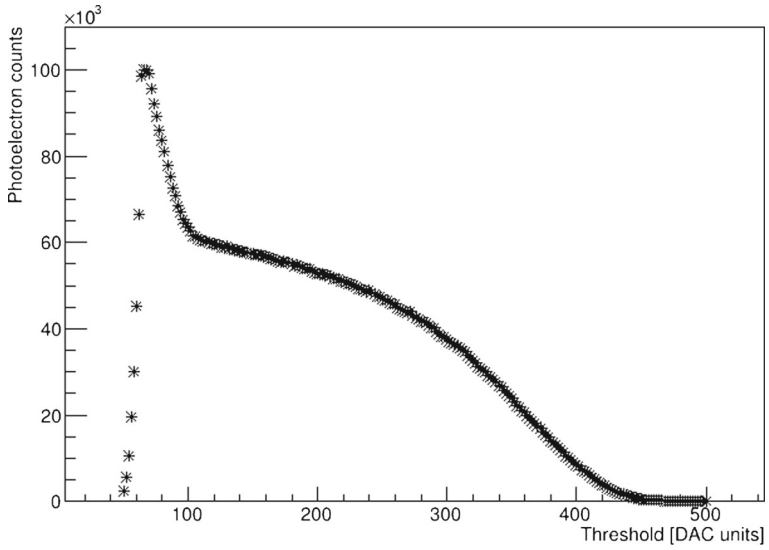

Fig. 5 A sample S-curve – sum of photon counts for specific number of measurements over the threshold for single photoelectron detection (in Digital to Analogue Converter (DAC) units)

approaches zero for high threshold values, above which there is nearly no signal. A sample S-curve can be seen on Fig. 5. "single photoelectron spectrum" is a derivative of an S-curve. It reveals separated peaks for the electronics noise – pedestal – and single photoelectron [8] (Fig. 6).

However, in our ASIC, a single threshold must be set for all pixels of a single PMT. Therefore the calibration procedure must determine an optimal amplifier gain for all pixels to have the same total gain, which roughly corresponds to obtaining a similar "single photoelectron spectrum" shape.[3] For this task the algorithm calculates the median position of the single photoelectron peak for all pixels and adjusts the gain of all pixels to move the peak to the median position. After the adjustment the measurement and median calculation is repeated to determine if the similarity of efficiency is satisfactory. If not, adjustment values are calculated and utilized again, until satisfactory performance is obtained.

3.2 Field calibration

The absolute calibration of the EUSO-TA can be also verified on-site by measuring bright reference stars, which provide a photon flux that is stable with a known UV spectrum at different elevation angles, which allows correcting for atmospheric attenuation.

In this configuration it is feasible to compare the night sky background measurements performed with EUSO-TA to the corresponding flux values obtained from

[3]The total gain of a pixel corresponds to the distance between the pedestal peak and the single photoelectron peak.

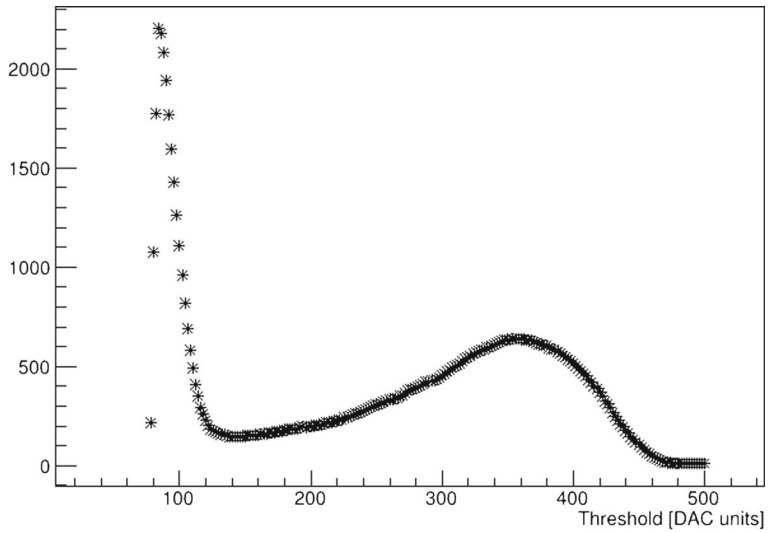

Fig. 6 A sample single pixel "single photoelectron spectrum" measured in laboratory, for threshold levels represented in DAC units. The noise peak on the left and single photoelectron peak on the right are clearly visible. The distance between peaks is determined by the total pixel gain. The minimum between the peaks is the single photoelectron valley – the optimal position of threshold for single photoelectron detection. Colored lines denote the threshold values, the rising slopes of the signal causing a detection and detections

the analysis of TA-FD data. Using a technique similar to that successfully used at the Pierre Auger Observatory [9], we superimpose views of the same sky region as observed by the EUSO-TA PDM and the TA-FD telescope. Precise alignment of EUSO-TA with TA-FD is possible by comparison of bright star trajectories crossing the field of views of both EUSO-TA and TA-FD.

The absolute night sky background flux observed by the two instruments looking toward the same sky direction (normalized to equal solid angle) provides a valuable tool for cross-calibration. In fact, an overlap of light curves from the diffuse component measured by two independent telescopes demonstrates the accuracy of the pixel-to-pixel variation correction.

One of the appealing features of this project is that EUSO-TA acquires data while running simultaneously with TA but without causing any interference with TA-FD operations. This offers the possibility to monitor the gain of individual camera pixels in realistic working condition, in which background flux can induce gain shifts. This monitoring can take place during the whole acquisition period, thus allowing detection of any eventual gain drift as well as verification of the linearity of pixel response in the range of variation of the night sky background.

Another advantage of the proposed method is that it allows eliminating completely any possible systematic error in relative calibration, particularly those induced by vignetting effects of the telescope optics at large off-axis angles. In fact, the whole telescope field of view can be compared in turn to the same reference instrument with a scan from the center to the periphery (if required). So, independent measurements of the night sky background flux can effectively be used as a general non-invasive

tool to verify the calibration of telescopes with large field of view and multi-pixel cameras.

Once the PDM is fully calibrated, the optics response can be characterized. In particular, the alignment, point spread function and lens transmitting efficiency can be measured and assessed with usual methods.

3.3 Cross-calibration using TA calibration facilities

The EUSO-TA telescope was installed at Black Rock Mesa (BRM) Station, about 100 m from the Electron Light Source (ELS). The ELS is a compact electron linear accelerator with a typical output of 10^9 electrons per pulse at 40 MeV, fired vertically in front of the detectors. It excites the atmosphere in a similar way to EAS, causing emission with the same spectrum, thus serving calibration purposes [10]. The second tool which will be used for cross-calibration of the detectors is the Central Laser Facility (CLF), distant from EUSO-TA by about 21 km. The CLF shoots vertically a laser of 355 nm wavelength in front of the detectors [11]. Both facilities are within the field of view of EUSO-TA.

3.4 Shower observation in coincidence

Figure 7 shows the location of the surface detectors (SDs) along the field of view of EUSO-TA. In the region contained within the dashed line, data obtained by TA-SD are also available and, therefore, extensive air showers landing in this region are

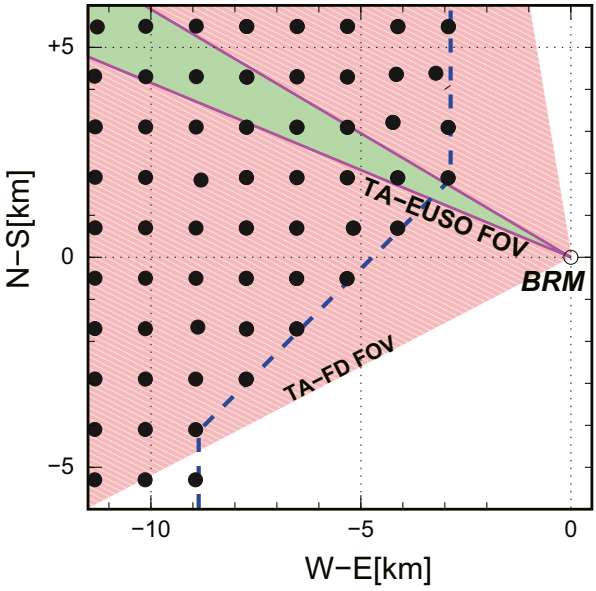

Fig. 7 Surface detector map near the BRM (Black Rock Mesa) station.The green area shows the EUSO-TA field of view. The red area shows the TA-FD field of view. EUSO-TA observes a part of the TA-FD field of view. On that direction, there are also the ELS station and CLF station of TA

the most useful events. For these events we expect the trigger to be issued by the TA-FD.

Figure 8 shows, from a detailed Monte Carlo simulation, the number of photoelectrons per 2.5 μs from 10^{18} eV showers with $\theta = 45°$ as a function of horizontal and vertical distances from BRM. The horizontal axis at the top represents the number of events per year within a threshold distance. The field of view of EUSO-TA is depicted as a sector viewing at a 25° elevation. The signal intensity N_{pe}, is evaluated using the following approximate formula:

$$N_{pe} \approx N_e \cdot FY \cdot T_{atm} \cdot \frac{A_{opt}\epsilon_{det}}{4\pi r^2} \cdot c \cdot t_{gate} \tag{1}$$

where N_e is the number of electrons on the shower axis at a distance r from the EUSO-TA telescope, FY is fluorescence yield, T_{atm} is the atmospheric transmittance along the line of site and t_{gate} is gate time. A_{opt} and ϵ_{det} are the effective aperture of the optics and overall detection efficiency of the MAPMTs, respectively.

The rate of events landing $\sim 3-4$ km from EUSO-TA (depending on the inclination angle), yielding more than 400 photoelectrons, is about 5 per year, while those landing around 9 km from the detector yielding about 100 photoelectrons are more frequent, about 50 per year. In the present estimation, we assume the UHECR spectrum reported by TA group at ICRC2011 [12] and a duty cycle of TA of ~ 10 %.

Figure 9 is a simulated example of an event distant from the detector by ~ 3 km (showing the images obtained by EUSO-TA and TA-FD). As the overall field of view of TA-FDs covers $3° - 31°$ in elevation, setting EUSO-TA elevation angle to $\sim 25°$ allows a direct cross-calibration using events with well-reconstructed geometries.

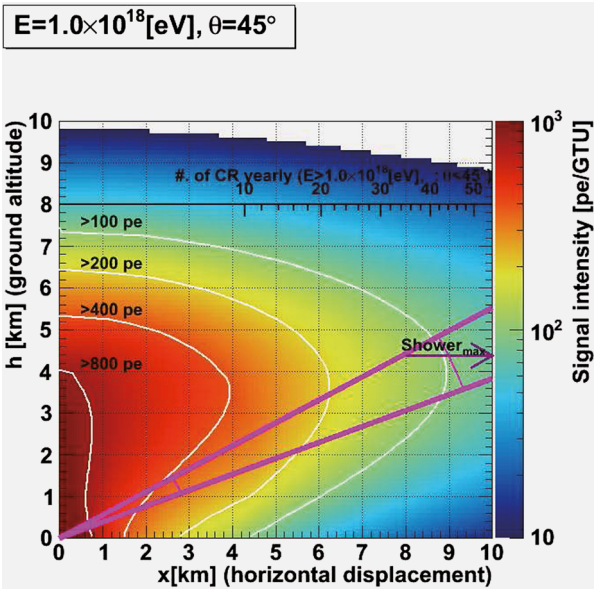

Fig. 8 Expected signal intensity (pe/2.5μs) from $10^{18} eV$ showers from $\theta = 45°$ as a function of horizontal distance and vertical distances. For the shower at the 6 km distance, we can observe about 200 pe/2.5μs

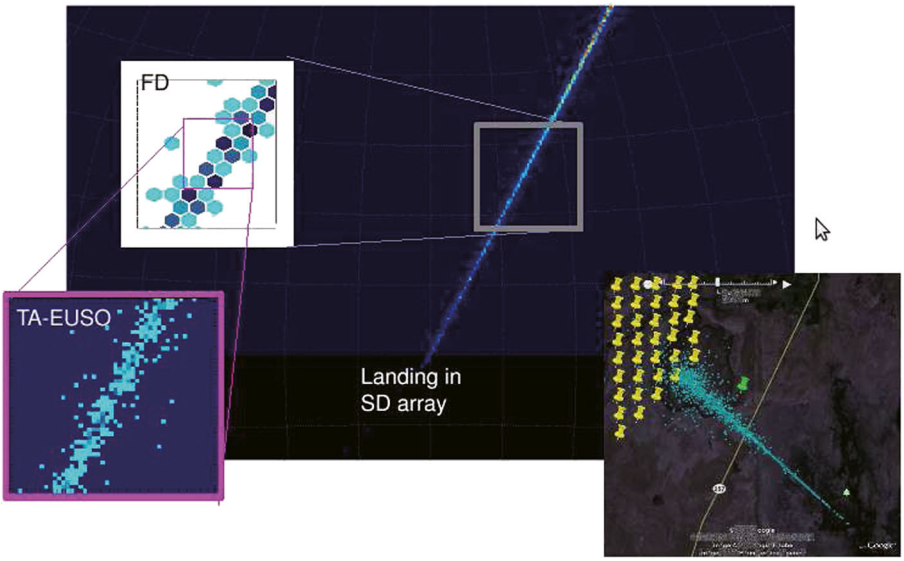

Fig. 9 A simulated example of an event close to the detector, yielding around 400 photoelectrons. The left windows show the pixel view of TA-FD and EUSO-TA

Moreover, EUSO-TA is capable of resolving the lateral distribution with tens-of-meter resolution when observing the EAS part close to its core. This will enable us to determine the lateral distribution near the core, complementing the SD measurements at several hundred meters to a few kilometers from the core. As the shower size which longitudinal development is measured by TA-FD is dominated by the particles near the core, such additional information will help to investigate the systematic uncertainties in energy scales of the SD relative to the FD measurements. We will also compare the data of EUSO-TA and TA-FD as well as signals from ELS and CLF.

4 Initial test at RIKEN

We have carried out initial tests of the integrated EUSO-TA at RIKEN institute, Wako-shi, Japan. The test setup included a focal surface consisting of two PMTs, the readout electronics, data acquisition and analysis software. First, we checked the apparatus response to an LED. All the components behaved as expected, properly sending and receiving internal commands and data allowed for storing and analysing the results. The apparatus demonstrated the expected reduction in the number of registered photoelectrons with increasing acceptance threshold. Also, the signal of the proper working range of the LED light, below the saturation level of the counting mode, has been obtained.

The second stage was a test of the apparatus behaviour in real conditions. The focal surface was integrated with the EUSO-TA lenses and pictures of the night sky were taken. Additionally, we tested the telescope response to a variable source. A moving UV laser spot was displayed on the wall in front of the detector and the

standard acquisition lasting a few seconds was performed. Analysis of the results show an increase followed by a decrease of the photon counts as the spot of the laser was moving in and out of the field of view (Fig. 10).

5 Initial test at TA site

We have installed the lenses of the telescope at TA site. To check the optics, we placed a simple detector in the focus. The detector consists of one EUSO-TA MAPMT and one Front-End ASIC. These are the same components as in the EUSO-TA electronics, and we were able to measure the luminosity using the photon counting method. We observed the night sky background with half moon, which was out of the field of view. We recorded 10 - 20 counts/2.5 μs (Fig. 11). This uncalibrated value is consistent with expectations for the night sky background in presence of moon [13] being 10-30 photons per EUSO-TA pixel depending on the exact pointing and the time of data taking.

6 Next steps

In near future we will start the final procedure of cross-calibration with the TA-FD telescope. This requires assembly of the whole focal surface consisting of 36 MAPMTs, initial tests of the detector response, and final tests under working conditions. Before the cross-calibration, we will need to perform an auto-calibration and fine-tuning of the detector to ensure the consistency in photoelectron counts between different parts of the focal surface. The next step will be to perform measurements of the night sky background and star light in different parts of the field of view and

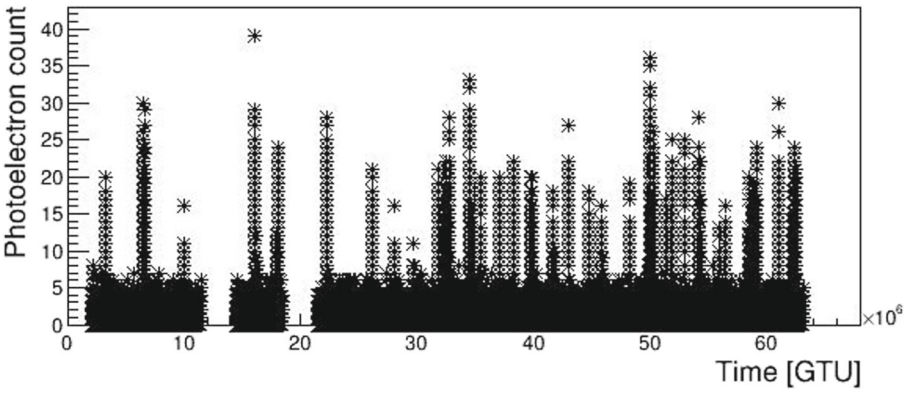

Fig. 10 The light curve (number of photoelectron counts vs time) of a $\sim$ 1 minute observation of a spot from a moving laser projected on a wall for a single pixel. The spot was periodically entering and exiting the field of view. The detector was not calibrated, therefore the photoelectron counts values presented are arbitrary

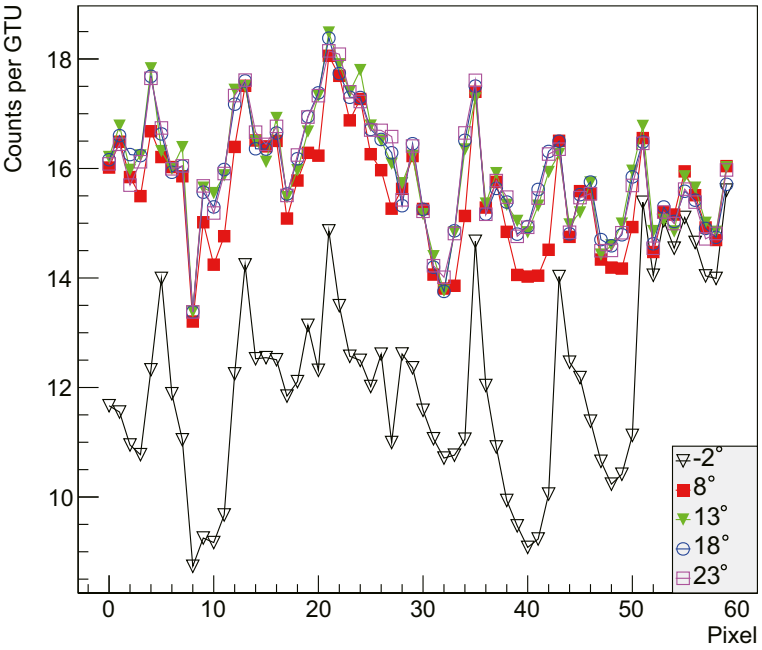

Fig. 11 Result of the measurement of the night sky background for various elevation angle

check consistency with models and calculation. After completion of these tasks we shall be able to acquire data simultaneously with the TA experiment and perform a meaningful comparison.

Acknowledgements This work was partially supported by Basic Science Interdisciplinary Research Projects of RIKEN and JSPS KAKENHI Grant (22340063, 23340081, and 24244042), by the Inter-University Research Program of the Institute for Cosmic Ray Research, by the Italian Ministry of Foreign Affairs, General Direction for the Cultural Promotion and Cooperation and by the 'Helmholtz Alliance for Astroparticle Physics HAP' funded by the Initiative and Networking Fund of the Helmholtz Association, Germany. LWP acknowledges support by JSPS.

References

1. Takahashi, Y., et al.: New J. Phys. **11**, 065009 (2009)
2. Kawai, H., et al.: Nucl. Phys. B (Proc. Suppl.) **175-176**, 221-226 (2008)
3. Prieto, H., et al.: Proceedings of 33rd International Cosmic Ray Conference, Rio de Janeiro 2013, arXiv:1307.7071, **95**
4. Miyamoto, H., et al.: Proceedings of 33rd International Cosmic Ray Conference, Rio de Janeiro 2013, arXiv:1307.7071, **103**
5. Bayer, J., et al.: Proceedings of 33rd International Cosmic Ray Conference, Rio de Janeiro 2013, arXiv:1307.7071, **99**
6. Kajino, F., et al.: Proceedings of 33rd International Cosmic Ray Conference, Rio de Janeiro 2013, arXiv:1307.7071, **11**

7. Gorodetzky, P., et al.: Proceedings of 33rd International Cosmic Ray Conference, Rio de Janeiro 2013, arXiv:1307.7071, **71**
8. Blaksley, C., Gorodetzky, P.: Nucl. Inst. Methods Phys. Res. Sec. A **764**, 198–205 (2014)
9. Segreto, A., et al.: Proceedings of 32nd International Cosmic Ray Conference, Beijing 2011 **3**, 129 (2011)
10. Shibata, T., et al.: Proceedings of 32nd International Cosmic Ray Conference, Beijing 2011 **3**, 1252
11. Takahashi, Y., et al.: AIP Conf. Proc. **1367**, 157 (2011)
12. Ivanov, D., et al.: Proceedings of 32nd International Cosmic Ray Conference, Beijing 2011 **2**, 258
13. Krisciunas, K., Schaefer, B.: Astronomical Society of the Pacific. Publications **103**, 1033–1039 (1991)

The JEM-EUSO Collaboration

J.H. Adams Jr.[md], S. Ahmad[bb], J.-N. Albert[ba], D. Allard[bc], L. Anchordoqui[mf], V. Andreev[me], A. Anzalone[dh,dn], Y. Arai[ev], K. Asano[et], M. Ave Pernas[kc], P. Baragatti[do], P. Barrillon[ba], T. Batsch[hc], J. Bayer[cd], R. Bechini[dl], T. Belenguer[kb], R. Bellotti[da,db], K. Belov[me], A.A. Berlind[mh], M. Bertaina[dk,dl], P.L. Biermann[cb], S. Biktemerova[ia], C. Blaksley[bc], N. Blanc[la], J. Błęcki[hd], S. Blin-Bondil[bb], J. Blümer[cb], P. Bobik[ja], M. Bogomilov[aa], M. Bonamente[md], M.S. Briggs[md], S. Briz[kd], A. Bruno[da], F. Cafagna[da], D. Campana[df], J-N. Capdevielle[bc], R. Caruso[dc,dn], M. Casolino[ew,di], C. Cassardo[dk,dl], G. Castellini[dd], C. Catalano[bd], O. Catalano[dh,dn], A. Cellino[dk,dm], M. Chikawa[ed], M.J. Christl[mg], D. Cline[me], V. Connaughton[md], L. Conti[do], G. Cordero[ga], H.J. Crawford[ma], R. Cremonini[dl], S. Csorna[mh], S. Dagoret-Campagne[ba], A.J. de Castro[kd], C. De Donato[di], C. de la Taille[bb], C. De Santis[di,dj], L. del Peral[kc], A. Dell'Oro[dk,dm] N. De Simone[di], M. Di Martino[dk,dm], G. Distratis[cd], F. Dulucq[bb], M. Dupieux[bd], A. Ebersoldt[cb], T. Ebisuzaki[ew], R. Engel[cb], S. Falk[cb], K. Fang[mb], F. Fenu[cd], I. Fernández-Gómez[kd], S. Ferrarese[dk,dl], D. Finco[do], M. Flamini[do], C. Fornaro[do], A. Franceschi[de], J. Fujimoto[ev], M. Fukushima[eg], P. Galeotti[dk,dl], G. Garipov[ic], J. Geary[md], G. Gelmini[me], G. Giraudo[dk], M. Gonchar[ia], C. González Alvarado[kb], P. Gorodetzky[bc], F. Guarino[df,dg], A. Guzmán[cd], Y. Hachisu[ew], B. Harlov[ib], A. Haungs[cb], J. Hernández Carretero[kc], K. Higashide[er,ew], D. Ikeda[eg], H. Ikeda[ep], N. Inoue[er], S. Inoue[eg], A. Insolia[dc,dn], F. Isgrò[df,dp], Y. Itow[en], E. Joven[ke], E.G. Judd[ma], A. Jung[fb], F. Kajino[ei], T. Kajino[el], I. Kaneko[ew], Y. Karadzhov[aa], J. Karczmarczyk[hc], M. Karus[cb], K. Katahira[ew], K. Kawai[ew], Y. Kawasaki[ew], B. Keilhauer[cb], B.A. Khrenov[ic], Jeong-Sook Kim[fa], Soon-Wook Kim[fa], Sug-Whan Kim[fd], M. Kleifges[cb], P.A. Klimov[ic], D. Kolev[aa], I. Kreykenbohm[ca], K. Kudela[ja], Y. Kurihara[ev], A. Kusenko[me], E. Kuznetsov[md], M. Lacombe[bd], C. Lachaud[bc], J. Lee[fc], J. Licandro[ke], H. Lim[fc], F. López[kd], M.C. Maccarone[dh,dn], K. Mannheim[ce], D. Maravilla[ga], L. Marcelli[dj], A. Marini[de], O. Martinez[gc], G. Masciantonio[di,dj], K. Mase[ea], R. Matev[aa], G. Medina-Tanco[ga], T. Mernik[cd], H. Miyamoto[ba], Y. Miyazaki[ec], Y. Mizumoto[el], G. Modestino[de], A. Monaco[da,db], D. Monnier-Ragaigne[ba], J.A. Morales de los Ríos[ka,kc], C. Moretto[ba], V.S. Morozenko[ic], B. Mot[bd], T. Murakami[ef], M. Nagano[ec], M. Nagata[eh], S. Nagataki[ek], T. Nakamura[ej], T. Napolitano[de], D. Naumov[ia], R. Nava[ga], A. Neronov[lb], K. Nomoto[eu], T. Nonaka[eg], T. Ogawa[ew], S. Ogio[eo], H. Ohmori[ew], A.V. Olinto[mb], P. Orleański[hd], G. Osteria[df], M.I. Panasyuk[ic], E. Parizot[bc], I.H. Park[fc], H.W. Park[fc], B. Pastircak[ja], T. Patzak[bc], T. Paul[mf], C. Pennypacker[ma], S. Perez Cano[kc], T. Peter[lc], P. Picozza[di,dj,ew], T. Pierog[cb], L.W. Piotrowski[ew], S. Piraino[cd,dh], Z. Plebaniak[hc], A. Pollini[la], P. Prat[bc], G. Prévôt[bc], H. Prieto[kc], M. Putis[ja], P. Reardon[md], M. Reyes[ke], M. Ricci[de], I. Rodríguez[kd], M.D. Rodríguez Frías[kc], F. Ronga[de], M. Roth[cb], H. Rothkaehl[hd], G. Roudil[bd], I. Rusinov[aa], M. Rybczyński[ha], M.D. Sabau[kb], G. Sáez Cano[kc], H. Sagawa[eg], A. Saito[ej], N. Sakaki[cb], M. Sakata[ei], H. Salazar[gc], S. Sánchez[kd], A. Santangelo[cd], L. Santiago Crúz[ga], M. Sanz Palomino[kb], O. Saprykin[ib], F. Sarazin[mc], H. Sato[ei], M. Sato[es], T. Schanz[cd], H. Schieler[cb], V. Scotti[df,dg], A. Segreto[dh,dn], S. Selmane[bc], D. Semikoz[bc], M. Serra[ke], S. Sharakin[ic], T. Shibata[eq], H.M. Shimizu[em], K. Shinozaki[ew,cd], T. Shirahama[er], G. Siemieniec-Oziębło[hb], H.H. Silva López[ga], J. Sledd[mg], K. Słomińska[hd], A. Sobey[mg], T. Sugiyama[em], D. Supanitsky[ga], M. Suzuki[ep], B. Szabelska[hc], J. Szabelski[hc], F. Tajima[ee], N. Tajima[ew], T. Tajima[cc], Y. Takahashi[es], H. Takami[ev], M. Takeda[eg], Y. Takizawa[ew], C. Tenzer[cd], O. Tibolla[ce], L. Tkachev[ia], H. Tokuno[et], T. Tomida[ew], N. Tone[ew], S. Toscano[lb], F. Trillaud[ga], R. Tsenov[aa], Y. Tsunesada[et], K. Tsuno[ew], T. Tymieniecka[hc], Y. Uchihori[eb], M. Unger[cb], O. Vaduvescu[ke], J.F. Valdés-Galicia[ga], P. Vallania[dk,dm], L. Valore[df,dg], G. Vankova[aa], C. Vigorito[dk,dl], L. Villaseñor[gb], P. von Ballmoos[bd], S. Wada[ew], J. Watanabe[el], S. Watanabe[es], J. Watts Jr.[md], M. Weber[cb], T.J. Weiler[mh], T. Wibig[hc],

L. Wiencke[mc], M. Wille[ca], J. Wilms[ca], Z. Włodarczyk[ha], T. Yamamoto[ei], Y. Yamamoto[ei], J. Yang[fb], H. Yano[ep], I.V. Yashin[ic], D. Yonetoku[ef], K. Yoshida[ei], S. Yoshida[ea], R. Young[mg], M.Yu. Zotov[ic], A. Zuccaro Marchi[ew]

[aa] St. Kliment Ohridski University of Sofia, Bulgaria
[ba] LAL, Univ Paris-Sud, CNRS/IN2P3, Orsay, France
[bb] Omega, Ecole Polytechnique, CNRS/IN2P3, Palaiseau, France
[bc] APC, Univ Paris Diderot, CNRS/IN2P3, CEA/Irfu, Obs. de Paris, Sorbonne Paris Cité, France
[bd] IRAP, Université de Toulouse, CNRS, Toulouse, France
[ca] ECAP, University of Erlangen-Nuremberg, Germany
[cb] Karlsruhe Institute of Technology (KIT), Germany
[cc] Ludwig Maximilian University, Munich, Germany
[cd] Inst. for Astronomy and Astrophysics, Kepler Center, University of Tübingen, Germany
[ce] Institut für Theoretische Physik und Astrophysik, University of Würzburg, Germany
[da] Istituto Nazionale di Fisica Nucleare - Sezione di Bari, Italy
[db] Universita' degli Studi di Bari Aldo Moro and INFN - Sezione di Bari, Italy
[dc] Dipartimento di Fisica e Astronomia - Universita' di Catania, Italy
[dd] Consiglio Nazionale delle Ricerche (CNR) - Ist. di Fisica Applicata Nello Carrara, Firenze, Italy
[de] Istituto Nazionale di Fisica Nucleare - Laboratori Nazionali di Frascati, Italy
[df] Istituto Nazionale di Fisica Nucleare - Sezione di Napoli, Italy
[dg] Universita' di Napoli Federico II - Dipartimento di Scienze Fisiche, Italy
[dh] INAF - Istituto di Astrofisica Spaziale e Fisica Cosmica di Palermo, Italy
[di] Istituto Nazionale di Fisica Nucleare - Sezione di Roma Tor Vergata, Italy
[dj] Universita' di Roma Tor Vergata - Dipartimento di Fisica, Roma, Italy
[dk] Istituto Nazionale di Fisica Nucleare - Sezione di Torino, Italy
[dl] Dipartimento di Fisica, Universita' di Torino, Italy
[dm] Osservatorio Astrofisico di Torino, Istituto Nazionale di Astrofisica, Italy
[dn] Istituto Nazionale di Fisica Nucleare - Sezione di Catania, Italy
[do] UTIU, Dipartimento di Ingegneria, Rome, Italy
[dp] DIETI, Universita' degli Studi di Napoli Federico II, Napoli, Italy
[ea] Chiba University, Chiba, Japan
[eb] National Institute of Radiological Sciences, Chiba, Japan
[ec] Fukui University of Technology, Fukui, Japan
[ed] Kinki University, Higashi-Osaka, Japan
[ee] Hiroshima University, Hiroshima, Japan
[ef] Kanazawa University, Kanazawa, Japan
[eg] Institute for Cosmic Ray Research, University of Tokyo, Kashiwa, Japan
[eh] Kobe University, Kobe, Japan
[ei] Konan University, Kobe, Japan
[ej] Kyoto University, Kyoto, Japan
[ek] Yukawa Institute, Kyoto University, Kyoto, Japan
[el] National Astronomical Observatory, Mitaka, Japan
[em] Nagoya University, Nagoya, Japan
[en] Solar-Terrestrial Environment Laboratory, Nagoya University, Nagoya, Japan
[eo] Graduate School of Science, Osaka City University, Japan
[ep] Institute of Space and Astronautical Science/JAXA, Sagamihara, Japan
[eq] Aoyama Gakuin University, Sagamihara, Japan
[er] Saitama University, Saitama, Japan
[es] Hokkaido University, Sapporo, Japan
[et] Interactive Research Center of Science, Tokyo Institute of Technology, Tokyo, Japan
[eu] University of Tokyo, Tokyo, Japan
[ev] High Energy Accelerator Research Organization (KEK), Tsukuba, Japan
[ew] RIKEN, Wako, Japan
[fa] Korea Astronomy and Space Science Institute (KASI), Daejeon, Republic of Korea
[fb] Ewha Womans University, Seoul, Republic of Korea
[fc] Sungkyunkwan University, Seoul, Republic of Korea
[fd] Center for Galaxy Evolution Research, Yonsei University, Seoul, Republic of Korea

[ga] Universidad Nacional Autónoma de México (UNAM), Mexico
[gb] Universidad Michoacana de San Nicolas de Hidalgo (UMSNH), Morelia, Mexico
[gc] Benemérita Universidad Autónoma de Puebla (BUAP), Mexico
[ha] Jan Kochanowski University, Institute of Physics, Kielce, Poland
[hb] Jagiellonian University, Astronomical Observatory, Krakow, Poland
[hc] National Centre for Nuclear Research, Lodz, Poland
[hd] Space Research Centre of the Polish Academy of Sciences (CBK), Warsaw, Poland
[ia] Joint Institute for Nuclear Research, Dubna, Russia
[ib] Central Research Institute of Machine Building, TsNIIMash, Korolev, Russia
[ic] Skobeltsyn Institute of Nuclear Physics, Lomonosov Moscow State University, Russia
[ja] Institute of Experimental Physics, Kosice, Slovakia
[ka] Consejo Superior de Investigaciones Científicas (CSIC), Madrid, Spain
[kb] Instituto Nacional de Técnica Aeroespacial (INTA), Madrid, Spain
[kc] Universidad de Alcalá (UAH), Madrid, Spain
[kd] Universidad Carlos III de Madrid, Spain
[ke] Instituto de Astrofísica de Canarias (IAC), Tenerife, Spain
[la] Swiss Center for Electronics and Microtechnology (CSEM), Neuchâtel, Switzerland
[lb] ISDC Data Centre for Astrophysics, Versoix, Switzerland
[lc] Institute for Atmospheric and Climate Science, ETH Zürich, Switzerland
[ma] Space Science Laboratory, University of California, Berkeley, USA
[mb] University of Chicago, USA
[mc] Colorado School of Mines, Golden, USA
[md] University of Alabama in Huntsville, Huntsville, USA
[me] University of California (UCLA), Los Angeles, USA
[mf] University of Wisconsin-Milwaukee, Milwaukee, USA
[mg] NASA - Marshall Space Flight Center, USA
[mh] Vanderbilt University, Nashville, USA